In vitro reconstitution of dynamic microtubules interacting with actin filament networks

Magdalena Preciado López[1], Florian Huber[1], Ilya Grigoriev[3], Michel O. Steinmetz[2], Anna Akhmanova[3], Marileen Dogterom[1]*, Gijsje H. Koenderink[1]*

[1] FOM Institute AMOLF, Science Park 104, 1098 XG, Amsterdam, The Netherlands.

[2] Laboratory of Biomolecular Research, Paul Scherrer Institut, CH-5232 Villigen PSI, Switzerland.

[3] Division of Cell Biology, Faculty of Science, Utrecht University, Padualaan 8, 3584 CH, Utrecht, The Netherlands.

* Correspondence to: dogterom@amolf.nl (M.D.), gkoenderink@amolf.nl (G.K.)

Abstract

Interactions between microtubules and actin filaments (F-actin) are essential for eukaryotic cell migration, polarization, growth and division. Although the importance of these interactions has been long recognized, the inherent complexity of the cell interior hampers a detailed mechanistic study of how these two cytoskeletal systems influence each other. In this paper we show how *in vitro* reconstitution can be employed to study how actin filaments and dynamic microtubules affect each other's organization. While we focus here on the effect of steric interactions, these assays provide an ideal starting point to develop more complex studies through the addition of known F-actin-microtubule cross-linkers, or myosin II motors.

Introduction

Interactions between microtubules and F-actin are essential for eukaryotic cells to execute processes such as migration, growth, division and polarization (as reviewed in *Yarm, Sagot & Pellman, 2003, Rodriguez, Schaefer, Mandato, Forscher, Bement & Waterman-Storer, 2003, Siegrist & Doe, 2007*). Historically, however, actin and microtubules have been mostly studied independently, even though the importance of their interactions has been long recognized (*Vasiliev, Gelfand, Domnina, Ivanova, Komm & Olshevskaja, 1970*). A chief obstacle in understanding how these cytoskeletal systems affect each other's organization lies in identifying when and where in the cell they interact. This is largely due to the inherent crowdedness of the cell, the high density and diversity of F-actin structures (stress fibers, filopodia, dendritic and cortical networks), and the complicated trajectories of polymerizing microtubules (Fig. 1A).

Furthermore, it is challenging to disentangle mechanical cross-talk from biochemical interactions (*Rodriguez et al, 2003*), mediated through cross-linking proteins or cytoskeletal regulators such as the Rho family of GTPases (*Waterman-Storer & Salmon, 1999, Etienne-Manneville & Hall, 2002*).

Notwithstanding, several proteins and protein complexes capable of linking microtubules to F-actin have been identified (Fig. 1C). Some of these form passive cross-links (*Geraldo, Khanzada, Parsons, Chilton & Gordon-Weeks, 2008, Solinet, Mahmud, Stewman, Ben el Kadhi, Decelle, Talje et al, 2013*); while others mediate active linkages, through molecular motors (*Yin, Pruyne, Huffaker & Brescher, 2000, Frey, Klotz & Nick, 2009, Nadar, Lin & Baas, 2012*), actin filament nucleators (*Mao, 2011, Shen, Hsiue, Sindelar, Welch, Campellone & Wang, 2012*), or proteins that localize to the growing plus ends of microtubules (+TIPs) (*Akhmanova & Steinmetz, 2008, Moseley, Bartolini, Okada, Wen, Gundersen & Goode, 2007, Jiang, Toedt, Montenegro Gouveia, Davey, Hua, van der Vaart et al, 2012, Wu, Kodama & Fuchs, 2008, Applewhite, Grode, Keller, Zadeh, Slep & Rogers, 2010, Lee, Tirnauer, Li, Schuyler, Liu et al, 2000*).

It is likely that in addition to the molecular properties of cross-linking proteins (Fig. 1C), the local cytoskeletal architecture (Fig. 1B) plays a defining role in the outcome of a given actin-microtubule interaction. For instance, we hypothesize that microtubule growth will respond differently to a dendritic F-actin network interspersed with filopodia than to a comparatively rigid actin stress fiber, even if the same cross-linking proteins are at play. Reconstituted model systems using purified cellular components are ideally suited to test such hypotheses, as they can separately address biochemical and mechanical interactions and identify the minimum requirements to achieve a certain functional organization. Not surprisingly, *in vitro* reconstitutions have played a fundamental role in our current understanding of the actin and microtubule cytoskeleton (as reviewed in *Dogterom & Surrey, 2013, Mullins & Hansen, 2013, Huber, Schnauß, Rönicke, Rauch, Müller, Fütterer et al, 2013*).

To date, however, reconstitutions of composite microtubule/F-actin systems are still rare. Notable exceptions include work on the mechanical properties of passive composite networks (*Brangwynne, Koenderink, MacKintosh & Weitz, 2008, Lin, Koenderink, MacKintosh & Weitz, 2010*), molecular motor motility and cargo transport at F-actin-microtubule cross-roads (*Ali, Krementsova, Kennedy, Mahaffy, Pollard, Trybus et al, 2007, Schroeder, Mitchell, Shuman, Holzbaur & Goldman, 2010*), and F-actin-microtubule co-bundling (*Selden & Pollard, 1986, Sider, Mandato, Weber, Zandy, Beach, Finst et al, 1999, Huang, Jin, Du, Li, Zha, Ou et al, 2007*). Given the mounting evidence that microtubule growing ends, through end-binding (EB) proteins, act as hubs of biochemical activity within the cell (*Lansbergen & Akhmanova, 2006, Akhmanova et al, 2008, Tamura & Draviam, 2012*), they are likely to play a defining role in the

regulation of actin-microtubule co-organization. However, with the exception of one study in *Xenopus laevis* egg extracts (*Waterman-Storer, Duey, Weber, Keech, Cheney, Salmon et al, 2000*), and some promising work coupling actin-filament nucleation to EBs (*Breitsprecher, Jaiswal, Bombardier, Gould, Gelles et al, 2012*), we are unaware of any *in vitro* reconstitution studies of the interaction between dynamic microtubules and F-actin.

In this paper we describe a set of assays that focus on steric interactions between dynamic microtubules and actin filaments arranged in pre-defined geometries. First, we address how microtubule growth and organization respond to quasi two-dimensional linear arrays of F-actin bundles (mimicking stress fibers); and second, how isotropic F-actin networks (mimicking cytosolic or cortical networks) respond to a radial array of microtubules growing within them. In both cases we include EB proteins, which autonomously enhance microtubule dynamics through increased growth speeds and catastrophe rates (*Vitre, Coquelle, Heichette, Garnier, Chretien & Arnal, 2008, Komarova, De Groot, Grigoriev, Gouveia, Munteanu, Schober et al, 2009*), while potentially sensitizing the microtubule tip to obstacles (*Janson, Dood & Dogterom, 2003*). We describe the procedures for reconstitution and fluorescence imaging, and provide suggestions on how to analyze the resulting actin-microtubule co-organization by automated image analysis. As explained in the outlook, this work provides a starting point for more complex assays including microtubule-actin cross-linkers such as the spectraplakins MACF/Shot (*Wu et al, 2008, Applewhite et al, 2010*) or the Myo2/Kar9 system of *Saccharomyces cerevisiae* (*Yin et al, 2000, Lee et al, 2000*).

Experimental Methods

1. Flow cell preparation

Both F-actin and microtubules are immobilized on thoroughly cleaned and functionalized glass coverslips.

1.1 Glass cleaning

We clean coverslips in ‘base piranha’ solution, a safer alternative to ‘acid piranha’ solution that only becomes reactive when heated to 60°C. Storing the cleaned coverslips in a 0.1M KOH aqueous solution activates OH groups on the glass surface (*Gell, Bormuth, Brouhard, Cohen, Diez, Friel et al, 2010*), giving the surface a net negative charge which is needed for later functionalization steps.

1. Under the fume-hood, mix Milli-Q water, 30% H_2O_2, and 30% NH_4OH at a 5:1:1 ratio in a glass beaker. The beaker should be large enough to fit a Teflon rack holding the coverslips, and filled with enough solution to fully cover the glass.

2. Heat to 75 °C on a hot plate with continuous stirring using a magnetic bar.
3. Place coverslips in the Teflon rack and rinse twice, 5 min each, with Milli-Q water (Merck Millipore, Billerica, MA, USA) in a bath sonicator.
4. Once the base piranha solution has reached a temperature of 75 °C (bubbles can be seen), insert the Teflon rack with the coverslips.
5. Incubate at 75 °C for 15 min in the fume-hood.
6. Rinse the coverslips as in step 3.
7. Store at room temperature (RT) in a 0.1 M KOH solution (for up to one month) until use.

Tip: 'Base piranha' is a dangerous reaction, so wear gloves and work carefully (*Thumser, McVittie, Latta & Tang*).
Tip: The 'base piranha' solution can be left in the hood overnight. At the end of the reaction, only water is left, which can be safely discarded down the sink.

The glass microscope slides can be cleaned in a less rigorous fashion:
1. Place the slides in a Teflon rack in a beaker with a 0.1 % (v/v) aqueous solution of Hellmanex™ and bath-sonicate for 20 min.
2. Rinse the slides twice in Milli-Q water, 5 min each, in a bath sonicator.
3. Sonicate the slides in 100% acetone for 20 min. Rinse.
4. Sonicate the slides in a 70% ethanol aqueous solution. Rinse.
5. Store at RT in a 0.1 M KOH solution until use.

1.2 Flow cell construction

We assemble flow cells with ~10 µl channels cut out from Parafilm® sandwiched between a cleaned glass slide and coverslip (Fig. 2A).

1. Rinse a clean glass slide and coverslip for 5 min in Milli-Q water, in a bath sonicator.
2. Using a glass slide as a ruler cut out three ~2 mm-wide and ~2.5 cm-long channels from Parafilm, spaced far enough that they will fit comfortably within a coverslip.
3. Blow-dry the glass with N_2 gas and place the Parafilm between coverslip and glass slide. Cut out excess film.
4. Melt the Parafilm on a 120 °C hot-plate for 10 seconds, while applying even pressure by placing a glass slide and small even metal surface on the coverslip.
5. Begin the surface functionalization right away (Section 4.1 or 5.1).

For assays in which we need to exchange the solutions during the experiment, we use glass-slides perforated with ~1 mm-diameter holes spaced 20 mm apart (to fit within a 2" coverslip, Fig. 2B). The Parafilm channels and coverslip are mounted on these glass slides such that the

holes become the entry and exit points of the channel. In this way, all solutions are flowed in and out from the side of the glass slide while the flow cell is mounted on the microscope stage (Fig. 3A).

2. Stabilized actin filaments and microtubule seeds

Traditionally, *in vitro* assays with F-actin and microtubules have been performed in radically different buffers (*Olmsted & Borisy, 1975, Pardee & Spudich, 1982*). We found that MRB80 (80 mM PIPES pH 6.8 with KOH, 1 mM EGTA and 4 mM $MgCl_2$), a variant of the well-known BRB80 buffer (*Brinkley, 1997*) typically used for microtubules, has sufficiently high ionic strength to trigger actin polymerization. Conversely, microtubule polymerization does not proceed in the canonical F-buffer (20 mM HEPES pH 7.4 with KOH, 1 mM EGTA, 2 mM $MgCl_2$ and 50mM KCl), likely due to the lower ionic strength and higher pH (*Olmsted et al, 1975*).

2.1 Phalloidin-stabilized actin filaments

We purify G-actin from rabbit skeletal muscle (*Gentry, van der Meulen, Noguera, Alonso-Latorre, Plastino & Koenderink, 2012)* and store it at 4 ^{o}C in G-buffer (2 mM Tris-HCl pH 7.8, 0.2 mM Na_2ATP, 0.2 mM $CaCl_2$, 5 mM dithiothreitol (DTT)). After four weeks, we clarify the protein by centrifugation at 149,000 g for 10 min and dialyze the supernatant overnight against G-buffer. In the assays, we use pre-polymerized F-actin containing a small fraction of G-actin labeled with Alexa Fluor® 488, 594 or 647 (Molecular Probes, Life Technologies, Carlsbad, CA, USA) (*Gentry et al, 2012*).

1. In G-buffer, prepare a G-actin mix (15% labeled protein) at a concentration such that the final G-actin concentration will be 1.5 µM (for experiments with F-actin bundles, Section 4) or 20 µM (for experiments with centrosomes, Section 5). Keep on ice.
2. In a separate tube, prepare an actin polymerization mix in MRB80 such that the final concentrations will be 5 mM DTT, phalloidin at a 1:1 molar ratio with G-actin, 50 mM KCl and 0.2 mM ATP.
3. Add the actin polymerization mix to the G-actin mix and incubate for 1 hour at room temperature (RT) in the dark, to avoid photo-bleaching.
4. The F-actin solution can be used for one week.

2.2 GMPCPP-stabilized microtubule seeds

We nucleate microtubules from surface-immobilized microtubule ‘seeds’. These seeds are biotinylated and stabilized against depolymerization with the slowly-hydrolyzable GTP analog guanylyl-(α,β)-methylene-diphosphonate (GMPCPP, *Hyman, Salser, Drechsel, Unwin & Mitchison, 1992*). For labeling we use TRITC Rhodamine, HiLyte® 488, or HiLyte® 635 and

biotin-labeled tubulins from Cytoskeleton Inc. (Denver, CO, USA). The following protocol gives short microtubule seeds (~ 5 µm in length).

1. Prepare a 20 µM tubulin mix (70% unlabeled, 12% fluorescent, and 18% biotinylated) in MRB80 on ice.
2. Spin down for 5 min at RT at 149,000 g.
3. Add GMPCPP to a final concentration of 1 mM.
4. Incubate at 37 °C for 30 min to induce polymerization.
5. Spin down as in step 2.
6. Resuspend the pellet in MRB80 to a final volume that corresponds to 20 µM tubulin, assuming that 80% of the tubulin is recovered.
7. Keep the solution of microtubule seeds in the dark at RT, and use within two days of preparation.

Tip: The most convenient way to spin down small volumes (5-200 µl) at high speeds is with an Airfuge$^{(R)}$ ultracentrifuge (Beckman Coulter, Brea, CA, USA). Depending on the rotor, the maximum speed (30 PSI) corresponds to ~149,000 g.

More stable seeds that can be frozen and stored at -80 °C can be obtained by cycling the microtubule seeds twice (*Gell et al, 2010*) to replace more of the GDP-tubulin with GMPCPP-tubulin. After thawing, we use these microtubule seeds for up to three days, since they anneal and get longer with time.

3. Microscopy and imaging

The best signal-to-noise ratio for *in vitro* surface assays with fluorescently-labeled proteins is achieved with total-internal reflection fluorescence (TIRF) microscopy. Since we must visualize two or even three proteins within one experiment, we use up to three different wavelengths: 488 nm, 561 nm and 635 nm (*Laan, Pavin, Husson, Romet-Lemonne, van Duijn, Preciado López et al, 2012)*. We obtain optimal fluorophore/laser combinations using TRITC Rhodamine-labeled tubulin, Alexa 647-labeled actin, and GFP-labeled EBs. If unlabeled EBs are used, Alexa 488-labeled G-actin works equally well.

We typically image microtubules at 2 s per frame with 100-200 ms exposure times. To ensure consistent microtubule dynamics and control the microtubule growth speed and average length (*Fygenson, Braun & Libchaber, 1994)*, we control the sample temperature with a home-built objective temperature controller with a range of 15-40 ± 1 °C.

4. Assay with randomly-oriented microtubule seeds and aligned F-actin

bundles

With this assay, one can probe how growing microtubules that are initially randomly oriented respond to a linear array of rigid F-actin bundles (organized by fascin, *Gentry et al, 2012*). We use flow cells with entry/exit points on the glass slide side (Fig. 2B), which allow us to sequentially flow in different solutions while monitoring the sample by TIRF microscopy (Fig. 2D).

4.1 Surface functionalization

We immobilize microtubule seeds on the coverslip surface via biotin-streptavidin (Fig. 2C, Top). We first coat the clean and negatively-charged glass (Section 1.1) with the block co-polymer poly(L-lysine)-graft-poly(ethylene glycol) functionalized with a biotin tag (PLL-PEG-Biotin). We then bind streptavidin, and coat hydrophobic patches with κ-casein and Pluronic® F-127. All solutions and rinsing steps are based on MRB80.

1. Prepare a flow cell from a clean coverslip and a glass slide with holes (Fig. 2B).
2. Flow in 0.2 mg/ml PLL-PEG-Biotin and incubate for 30-45 min.
3. Rinse with 4-5 channel volumes (CVs).
4. Flow in 50 - 100 µg/ml streptavidin, incubate for 10 min. Rinse.
5. Flow in 0.5 mg/ml κ-casein, incubate for 10 min. Rinse.
6. Flow in 1% (w/v) Pluronic® F-127, incubate for 10 min. Rinse. Now the flow cell is ready for use.

Tip: To avoid drying of the channels during incubation steps, place the flow cell in a Petri-dish along with tissue paper soaked in water.
Tip: Streptavidin can be replaced with NeutrAvidin^{TM}.

4.2 Surface deposition of microtubule seeds and F-actin bundles

Before adding the microtubule polymerization mix to the flow-cell, we prepare the surface with randomly oriented microtubule seeds and aligned F-actin bundles (Fig. 2E). During each step, F-actin bundle formation is monitored by TIRF microscopy (Fig. 2D). All rinsing steps are with MRB80.

1. Flow in microtubule seeds diluted to an equivalent of 50-100 nM tubulin in MRB80 with 0.1% (w/v) methyl-cellulose, which exerts an entropic force pushing the seeds towards the surface. Incubate for 2 min.
2. Gently rinse with 2 CVs.
3. Flow in phalloidin-stabilized actin filaments at the equivalent of 1 µM G-actin in MRB80 containing 0.2% (w/v) methyl-cellulose, which is sufficient to push the filaments towards the

surface without inducing bundle formation (*Popp, Yamamoto, Iwasa & Maéda, 2006*).

4. Place a drop of 0.5 % (w/v) methyl-cellulose at one end of the channel and let it diffuse in for 5 min; this will induce F-actin bundling and cause a pressure-driven flow that aligns the bundles.
5. Slowly rinse the channel with 3 CVs of a solution containing 200 nM fascin and 0.1% (w/v) methyl-cellulose. This will stabilize the F-actin bundles and remove excess methyl-cellulose. Since fascin exchanges quickly (*Courson & Rock, 2010*), always keep its concentration constant in the channel to maintain the F-actin bundles.

Tip: In step 2, rinse slowly, to prevent attachment and alignment of freely-floating microtubule seeds on the surface.

Tip: Pipette F-actin solutions with a pipette tip whose tip is cut off, to avoid filament breakage.

Tip: Letting the sample equilibrate for ~ 10-20 min after fascin addition leads to more needle-like F-actin bundles (Fig. 2E).

Tip: Note that the density and degree of alignment of the F-actin bundles typically vary across the flow chamber, so regions of interest should be picked with care.

4.3 Dynamic microtubules growing within F-actin bundle arrays

A minimal mixture for microtubule polymerization should contain tubulin, GTP, a blocking agent, an oxygen scavenging system to prevent photo-damage and a reducing agent. Additionally, we add EB3 (EB family member 3, purified as in *Komarova et al, 2009* and *Montenegro Gouveia, Leslie, Kapitein, Buey, Grigoriev et al, 2010*), and use KCl to tune EB3's microtubule tip and lattice binding affinities. Methylcellulose is included to confine out-of-plane microtubule fluctuations, as needed for TIRF microscopy.

1. Make the following mixture in MRB80, keep on ice:
    - 0.1% methylcellulose
    - 0.2 mg/ml κ-casein
    - Oxygen scavenging and reducing cocktail (0.2 mg/ml catalase, 0.4 mg/ml glucose oxidase, 4 mM DTT)
    - 50 mM glucose
    - 50 mM KCl
    - 1 mM GTP
    - 100 nM EB3
    - 0.5 µM fascin
    - 23 µM unlabeled tubulin
    - 2 µM TRITC Rhodamine-labeled tubulin

2. Clarify the mixture at ~ 149,000 g for 5 min and immediately add to flow cell.
3. Seal the channel with vacuum grease or wax to prevent solvent evaporation.

Tip: An alternative oxygen scavenging system consists of protocatechuate 3,4-dioxygenase (PCD) and protocatechuic acid (PCA), which has the advantage that it does not acidify over time (*Shi, Lim & Ha, 2010*).

Tip: Higher tubulin concentrations will yield a larger microtubule growth speed and average length (*Fygenson et al, 1994*). Since longer microtubules align better with the F-actin bundles, tubulin concentrations ≥ 25 μM work best.

Tip: The concentration of EB proteins is chosen to enhance the ratio of microtubule tip over lattice binding (*Bieling, Laan, Schek, Munteanu, Sandblad, Dogterom et al, 2007*).

Tip: Additional proteins such as +TIPs, actin-binding proteins, or F-actin-microtubule cross-linkers can be included in the microtubule polymerization mix.

4.4 F-actin bundle and microtubule orientation analysis

We quantify the degree of F-actin-microtubule co-alignment by analyzing the local anisotropy in fluorescence intensity for all image pixels using the OrientationJ plugin (*Rezakhaniha, Agianniotis, Schrauwen, Griffa, Sage, Bouten et al, 2012*) developed for ImageJ (*Rasband, 2012*). This plugin calculates the spatial gradients of the fluorescence intensity within a user-defined window centered on each pixel. The dominant orientation of a pixel is given by the direction of minimum change in intensity. In addition, the plugin returns the coherency of each pixel, i.e. the degree of co-alignment of a pixel with its neighbors. We use the Gaussian gradient analysis method with a window size of two pixels; this combination reduces artifacts and the contribution of noise to the orientation measurements (*Alvarado, Mulder & Koenderink, 2013*).

Finally we construct orientation histograms for the microtubules and F-actin bundles by weighting the orientation values by the coherency. Figure 3C shows an example of a time-lapse experiment, where we automatically track microtubule co-alignment with F-actin bundle arrays of three different densities. Figure 3D shows the resulting orientation histograms for the microtubules at the start and the end (~ 1.5 hr) of the experiment. At all F-actin densities, the orientation distributions are initially rather random. However, only at the higher bundle densities, the microtubule orientation distributions develop a clear peak at an angle close to the average direction of the actin bundles. The higher the density of the actin bundle array, the stronger the degree of co-alignment. This finding suggests that steric interactions can drive actin-microtubule co-alignment, which may act in concert with specific interactions mediated by F-actin-microtubule cross-linkers such as the MACF/EB complex, which is thought to mediate microtubule alignment with actin stress fibers (*Wu et al, 2008*).

5. Radial arrays of microtubules growing within isotropic F-actin networks

This assay probes how a radial array of dynamic microtubules (nucleated by a centrosome) interacts with an entangled meshwork of actin filaments (Fig. 2C, bottom). Although we focus here on how the F-actin network responds to microtubules growing within it, we are also using this assay to study how microtubule growth responds to a decreasing mesh sizes of the actin meshwork (to be published elsewhere).

5.1 Surface preparation

1. Prepare a flow cell (Section 1 and Fig. 2A).
2. Pre-warm the centrosomes to 37 °C for 10 min and gently dilute them with MRB80 at RT. We purify centrosomes from KE37 cells and store them at -80°C in a 30% sucrose solution (*Laan et al, 2012*).
3. Add centrosomes to the flow cell. Wait 5 min to allow for surface adhesion.
4. Rinse with 5-10 CVs of MRB80.
5. Flow in a 0.2 mg/ml PLL-PEG solution. Incubate 10 min.
6. Rinse with 5-10 CVs of a 1 mg/ml κ-casein and 1% Pluronic® F-127 solution. Incubate 15 min.
7. Rinse with a 1 mg/ml κ-casein solution.

Tip: Since centrosomes are non-specifically bound to the glass, any contaminating proteins will bind as well. To prevent protein aggregates on the surface, substantial rinsing in step 4 is essential to achieve satisfactory passivation in later steps.

Tip: After step 6, samples can be stored on ice, but immediate use is recommended since the ability of centrosomes to nucleate microtubules deteriorates.

5.2 Dynamic microtubule assay within entangled actin filament networks

We use a similar polymerization mixture as in Section 4, but in this case phalloidin-stabilized actin filaments are included, and fascin is left out.

1. Prepare the following mix in MRB80:
   - 0.1% (w/v) methylcellulose
   - 1 mg/ml κ-casein
   - Oxygen scavenging and reducing cocktail
   - 50 mM glucose
   - 50 mM KCl
   - 1 mM GTP
   - 16-30 µM tubulin (1:15 labeled to unlabeled subunits)
   - 100-200 nM EB3

- 1-10 µM phalloidin-stabilized F-actin

2. After mixing, immediately add to the flow-cell channel and seal to prevent solvent evaporation.

> **Tip**: Higher tubulin concentrations facilitate microtubule nucleation and growth at lower temperatures (e.g. 30 µM tubulin at 25 °C). For lower tubulin concentrations, higher temperatures may be needed (e.g. 15-20 µM tubulin at 30 °C).
> **Tip**: We use actin concentrations between 1-10 µM, which is sufficient for filaments to entangle. At concentrations above 48 µM, the filaments form a nematic phase (*Käs, Strey, Tang, Finger, Ezzell, Sackmann et al, 1996*).

5.3 Analysis of local changes in F-actin network density

At the start of these experiments we typically observe a depletion of F-actin in close vicinity to the centrosome (Fig. 4A). This depletion zone closes over time as the actin filaments diffuse inward. With the use of a MATLAB (MathWorks Inc., Natick, MA, USA) script, we can quantify the time-scale of 'F-actin invasion' by measuring the average F-actin fluorescence intensity profile along circles of increasing radius centered about the centrosome position. The resulting radial intensity profiles show that the actin filaments reach a fairly homogeneous distribution within 15-30 min (Fig. 4B). This time scale is consistent with the typical time scale of actin filament diffusion by reptation observed previously at comparable F-actin concentrations (*Käs et al, 1996*). Figure 4C shows a typical example of the steady-state arrangement of microtubules and actin filaments after equilibration. The actin filaments appear unperturbed by the microtubules growing into the network, and conversely, the microtubules appear to grow unhampered.

Outlook

In this paper we introduced methods that allow for the simultaneous reconstitution of dynamic microtubules and actin networks. By pre-organizing the actin network in different ways, either in parallel bundles or in loosely connected networks, we show that microtubules and actin can influence each other's organization and dynamics in different ways, purely as a result of steric effects. In our lab, we are using these assays as a starting point for mechanistic studies of the effect of specific crosslinking proteins on the co-organization of actin and microtubule networks (to be published elsewhere). As a preliminary example, we show in Figure 4D how individual filaments in a loose actin network can become radially organized by a dynamic aster of microtubules in the presence of an F-actin-binding +TIP protein.

Reagents and stocks

Here we provide a list of key reagents and stock solutions in alphabetical order. Unless stated otherwise, chemicals were obtained from Sigma and stock solutions are prepared in MRB80. For stock solutions, information is provided as follows: name (catalog number, company), concentration, optional details, storage temperature.

- ATP (disodium salt hydrate, A2383), 50mM, -80 °C
- D-Glucose (G7528), 1M, filter, -80 °C
- G-actin (labeled and unlabeled), for long term storage keep concentration ≥ 48 µM in G-buffer, -80 °C
- Alexa Fluor® 488, Alexa Fluor® 594, and Alexa Fluor® 647succinimidyl ester dyes (A-20000, A-20004, A-20006, Molecular Probes, Life Technologies, Carlsbad, CA, USA), -20 °C
- GMPCPP (10mM solution, NU-405, Jena Biosciences, Jena, Germany), -80 °C
- GTP (G8877), 50mM, -80 °C
- H_2O_2 (30% in water, non-stabilized, 95313), 4 °C
- κ-casein (C0406), 5 mg/ml, filter, -80 °C
- Methyl-cellulose (M0512), 1% (w/v), -80 °C
- NeutrAvidin™ (31055, Thermo Scientific, Pierce Protein Biology Products, Rockford, IL, US), 5 mg/ml, -80 °C
- NH_4OH (30% in water, 320145), RT
- Oxygen scavenging and reducing cocktail (50X): 200 mM DTT, 10 mg/ml catalase and 20 mg/ml glucose oxidase in MRB80, filter, -80 °C
- DTT (D0632), 1M, -80 °C
- Catalase (powder, C9322), -20 °C
- Glucose oxidase (powder, G7016), -20 °C
- Phalloidin (P2141), 1mM in methanol, -20 °C
- PLL-PEG (PLL(20)-g[3.5]- PEG(2), Susos AG, Dübendorf, Switzerland), 2mg/ml, -80 °C
- PLL-PEG-Biotin (PLL(20)-g[3.5]-PEG(2)/PEG(3.4)-Biotin (50%), Susos AG), 2 mg/ml, -80 °C
- Pluronic® F-127 (P2443), 10% (w/v) in DMSO, RT
- Streptavidin (85878), 5 mg/ml, -80 °C
- Tubulin (T240, Cytoskeleton Inc., Denver, CO, USA), 50 µM, -80 °C
- Tubulin HiLyte 488-labeled, HiLyte 647-labeled, TRITC Rhodamine-labeled, and Biotin-labeled (TL488M, TL670M, TL590M, T333P Cytoskeleton Inc), 50 µM, -80 °C

References

Akhmanova, A., Steinmetz, M.O. (2008). Tracking the ends: a dynamic protein network controls the fate of microtubule tips. *Nat. Rev. Mol. Cell Biol*. **9**, 309-322.

Ali. M.Y., Krementsova, E.B., Kennedy, G.G., Mahaffy, R., Pollard, T.D., Trybus, K.M., Warshaw, D.M. (2007). Myosin Va maneuvers through actin intersections and diffuses along microtubules. *Proc. Natl. Acad. Sci. U.S.A.* **104** (11), 4332-4336.

Alvarado, J., Mulder, B.M., Koenderink, G.H. (2013). Alignment of nematic and bundled semiflexible polymers in cell-sized confinement. *Soft Matter*, in print.

Applewhite, D.A., Grode, K.D., Keller, D., Zadeh, A.D., Slep, K.C., Rogers, S.L. (2010). The spectraplakin Short stop is an actin-microtubule cross-linker that contributes to organization of the microtubule network. *Mol. Biol. Cell* **21** (10), 1714-1724.

Bieling, P., Laan, L., Schek, H., Munteanu, L., Sandblad, L., Dogterom, M., Brunner, D., Surrey, T. (2007). Reconstitution of a microtubule plus-end tracking system *in vitro*. Nature 450, 1100-1105.

Brangwynne, C., Koenderink, G., MacKintosh, F., Weitz, D. (2008). Nonequilibrium microtubule fluctuations in a model cytoskeleton. *PRL* **100**, 118104

Breitsprecher, D., Jaiswal, R., Bombardier, J.P., Gould, C.J., Gelles, J., Goode, B.L. (2012). Rocket launcher mechanism of collaborative actin-assembly defined by single-molecule imaging. *Science* **336**, 1164-1168.

Courson, D.S., Rock, R.S. (2010). Actin cross-link assembly and disassembly mechanics for apha-actinin and fascin. J. Biol. Chem. 285, 26350-26357.

Dogterom, M., Surrey, T. (2013). Microtubule organization *in vitro*. *Curr. Opin. Cell Biol.* **25** (1), 23-29.

Etienne-Manneville, S., Hall, A. (2002). Rho GTPases in cell biology. *Nature* **420**, 629-635.

Frey, N., Klotz, J., Nick, P. (2009). Dynamic bridges – a calponin-domain kinesin from rice links actin filaments and microtubules in both cycling and non-cycling cells. *Plant Cell Physiol.* **50**, 1493-1506.

Fygenson, D.K., Braun, E., Libchaber, A. (1994). Phase diagram of microtubules. Phys. Rev. E 50 (2), 1579-1588.

Gell, C., Bormuth, V., Brouhard, G.J., Cohen, D.N., Diez, S., Friel, C.T., Helenius, J., Nitzsche, B., Petzold, H., Ribbe, J., Schaeffer, E., Stear, J.H., Trushko, A., Varga, V., Widlund, P.O., Zanic, M., Howard, J. (2010). Microtubule dynamics reconstituted *in vitro* and imaged by single-molecule fluorescence microscopy. In L. Wilson & J.J. Correia (Vol. Eds.), *Methods in Cell Biology:* Vol. 95, Ch. 13 (p.p. 221-245). Amsterdam: Elsevier.

Gentry, B. S., van der Meulen, S., Noguera, P., Alonso-Latorre, B., Plastino, J., Koenderink, G.H. (2012). Multiple actin binding domains of Ena/VASP proteins determine actin network stiffening. *Eur. Biophys. J.* **41**, 979-990.

Geraldo, S., Khanzada, U.K., Parsons, M., Chilton, J.K., Gordon-Weeks, P.R. (2008). Targeting of the F-actin-binding protein drebrin by the microtubule plus-tip protein EB3 is required for neuritogenesis. *Nat. Cell Biol.* **10**, 1181-1189.

Huang, S.F., Jin, L.F., Du, J.Z., Li, H., Zha, Q., Ou, G.S., Ao, G.M., Yuan, M. (2007). SB401, a pollen-specific protein from *Solanum berthaultii*, binds to and bundles microtubules and F-actin. *Plant J.* **51**, 406-418.

Huber, F., Schnauß, J., Rönicke, S., Rauch, P., Müller, K., Fütterer, C., Käs, J. (2013). Emergent complexity of the cytoskeleton: from single filaments to tissue. *Adv. Phys.* **62** (1), 1-112.

Hyman, A.A., Salser, S., Drechsel, D.N., Unwin, N., Mitchison, T.J. (1992). Role of GTP hydrolysis in microtubule dynamics: information from a slowly hydrolysable analogue, GMPCPP. *Mol. Biol. Cell* **3** (10), 1155-1167.

Jiang, K., Toedt, G., Montenegro Gouveia, S., Davey, N.E., Hua, S., van der Vaart, B., Grigoriev, I., Larsen, J., Pedersen, L.B., Bezstarosti, K., Lince-Faria, M., Demmers, J., Steinmetz, M.O., Gibson, T.J., Akhmanova, A. (2012). A Proteome-wide screen for mammalian SxIP motif-containing microtubule plus-end tracking proteins. *Curr. Biol.* **22** (19), 1800-1807.

Käs, J., Strey, H., Tang, J.X., Finger, D., Ezzell, R., Sackmann, E., Janmey, P.A. (1996). F-actin, a model polymer for semiflexible chains in dilute, semidilute, and liquid crystalline solutions. *Biophys. J.* **70** (2), 609-625.

Laan, L., Pavin, N., Husson, J., Romet-Lemonne, G., van Duijn, M., Preciado López, M., Vale, R.D., Jülicher, F., Reck-Peterson, S.L., Dogterom, M. (2012). Cortical dynein controls microtubule dynamics to generate pulling forces that position microtubule asters. *Cell* **148**, 502-

514.

Lansbergen, G., Akhmanova, A. (2006). Microtubule plus end: a hub of cellular activities. *Traffic* **7**, 499-507.

Lee, L., Tirnauer, J.S., Li, J., Schuyler, S.C., Liu, J.Y., Pellman, D. (2000). Positioning of the mitotic spindle by a cortical-microtubule capture mechanism. *Science* **287**, 2260-2262.

Lin, Y-C. Koenderink, G.H., MacKintosch, F.C., Weitz, D.A. (2010). Control of non-linear elasticity in F-actin networks with microtubules. Soft Matter 7, 902-906.

Mao, Y. (2011). FORMIN a link between kinetochores and microtubule ends. *Trends Cell Biol.* **21** (11), 625-629.

Montenegro Gouveia, S., Leslie, K., Kapitein, L.C., Buey, R.M., Grigoriev, I., Wagenbach, M., Smal, I., Meijering, E., Hoogenraad, C.C., Wordeman, L., Steinmetz, M.O., Akhmanova, A. (2010). In vitro reconstitution of the functional interplay between MCAK and EB3 at microtubule plus ends. *Curr. Biol.* **20**, 1717-1722.

Moseley, J.B., Bartolini, F., Okada, K., Wen, Y., Gundersen, G.G., Goode, B.L. (2007). Regulated binding of adenomatous polyposis coli protein to actin. *J. Biol. Chem.* **282** (17), 12661-12668.

Mullins, R.D., Hansen, S.D. (2013). *In vitro* studies of actin filament network dynamics. *Curr. Opin. Cell Biol.* **25** (1), 6-13.

Nadar, V.C., Lin, S., Baas, P.W. (2012). Microtubule redistribution in growth cones elicited by focal inactivation of kinesin-5. *J. Neurosci.* **32** (17), 5783-5794.

Olmsted, J.B., Borisy, G.G. (1975). Ionic and nucleotide requirements for microtubule polymerization *in vitro*. *Biochem.* **14** (13), 2996-3005.

Pardee, J.D., Spudich, J.A. (1982). Mechanism of K+-induced actin assembly. *J. Cell. Biol.* **93**, 648-654.

Popp, D., Yamamoto, A., Iwasa, M., Maéda, Y. (2006). Direct visualization of actin nematic network formation and dynamics. *Biochem. Biophys. Res. Commun.* **351** (2), 348-353.

Rasband, W. S. ImageJ, U. S. National Institutes of Health, Bethesda, Maryland, USA, http://imagej.nih.gov/ij, 1997-2012.

Rezakhaniha, R., Agianniotis, A., Schrauwen, J.T., Griffa, A., Sage, D., Bouten, C.V., van de Vosse, F.N., Unser, M., Stergiopulos, N. (2012). Experimental investigation of collagen waviness and orientation in the arterial adventitia using confocal laser scanning microscopy. *Biomech. Model. Mechan.* **11**, 461-473.

Rodriguez, O.C., Schaefer, A. W., Mandato, C.A., Forscher, P., Bement, W.M., Waterman-Storer, C. M. (2003). Conserved microtubule-actin interactions in cell movement and morphogenesis. *Nat. Rev. Mol. Cell Biol.* **5**, 599-609.

Schroeder, H.W. III, Mitchell, C., Shuman, H., Holzbaur, E.L., Goldman, Y.E. (2010). Motor number controls cargo switching at actin-microtubule intersections *in vitro*. *Curr. Biol.* **20** (8), 687-696.

Selden, S.C., Pollard, T.D. (1986). Interaction of actin filaments with microtubules is mediated by microtubule-associated proteins and regulated by phosphorylation. *Ann. N.Y. Acad. Sci.* **466**, 803-812.

Shen, Q.T., Hsiue, P.P., Sindelar, C.V., Welch, M.D., Campellone, K.G., Wang, H.W. (2012). Structural insights into WHAM-mediated cytoskeletal coordination during membrane remodeling. *J. Cell Biol.* **199** (1), 111-124.

Shi, X., Lim, J., Ha, T. (2010). Acidification of the oxygen scavenging system in single-molecule fluorescence studies: In situ sensing with ratiometric dual-emission probe. Anal. Chem. 82 (14), 6132-6138.

Sider, J.R., Mandato, C.A., Weber, K.L., Zandy, A.J., Beach, D., Finst, R.J., Skoble, J., Bement, W.M. (1999). Direct observation of microtubule-f-actin interaction in cell free lysates. *J. Cell Sci.* **112**, 1947-1956.

Siegrist, S.E., Doe, C.Q. (2007). Microtubule-induced cortical cell polarity. *Genes & Dev.* **21**, 483-496.

Solinet, S., Mahmud, K., Stewman, S.F., Ben El Kadhi, K., Decelle, B., Talje, L., Ma, A., Kwok, B.H., Carreno, S. (2013). The actin-binding ERM protein Moesin binds to and stabilizes microtubules at the cell cortex. *J. Cell. Biol.* **202** (2), 251-260.

Tamura, N., Draviam, V.M. (2012). Microtubule plus-ends within a mitotic cell are 'moving platforms' with anchoring, signaling and force-coupling roles. *Open Biol.* 2, 120132.

Vasiliev, M., Gelfand, I.M., Domnina, L.V., Ivanova, O.Y., Komm, S.G., Olshevskaja, L.V. (1970). Effect of colcemid on the locomotory behavior of fibroblasts. *J. Embryol. Exp. Morph.* **24** (3), 625-640.

Vitre, B., Coquelle, F.M., Heichette, C., Garnier, C., Chretien, D., Arnal, I. (2008). EB1 regulates microtubule dynamics and tubulin sheet closure *in vitro*. Nat. Cell Biol. 10, 415-421.

Waterman-Storer, C.M., Salmon, E.D. (1999). Positive feedback between microtubule and actin dynamics during cell motility. *Curr. Opin. Cell Biol.* **11**, 61-67.

Waterman-Storer, C., Duey, D.Y., Weber, K.L., Keech, J., Cheney, R.E., Salmon, E.D., Bement, W.M. (2000). Microtubules remodel actomyosin networks in *Xenopus* egg extracts via two mechanisms of F-actin transport. *J. Cell Biol.* **150** (2), 361-376.

Wu, X. Kodama, A. Fuchs, E. (2008). ACF7 regulates cytoskeletal-focal adhesion dynamics and migration and has ATPase activity. *Cell* **135** (1), 137-148.

Yarm, F., Sagot, I., Pellman, D. (2001). The social life of actin and microtubules: interaction versus cooperation. *Curr. Opin. Microbiol.* **4** (6), 696-702.

Yin, H., Pruyne, D., Huffaker, T.C., Brescher, A. (2000). Myosin V orientates the mitotic spindle in yeast. *Nature* **406**, 1013-1015.

Acknowledgments:
We are grateful to K.L. Yu, B. van der Vaart and K. Jiang for help with cloning, C. Manatschal for help with protein purification and D. Mullins for providing us with the fascin plasmid. We thank B. Mulder and J. Alvarado for advice with the orientation analysis and K. Taute and N. Kurniawan for helpful comments on the manuscript. This work is part of the research program of the Foundation for Fundamental Research on Matter (FOM), which is part of the Netherlands Organization for Scientific Research (NWO). FH was supported by a Marie Curie fellowship. The data reported in this manuscript are all contained in the main paper and in the supplementary materials.

Figure captions

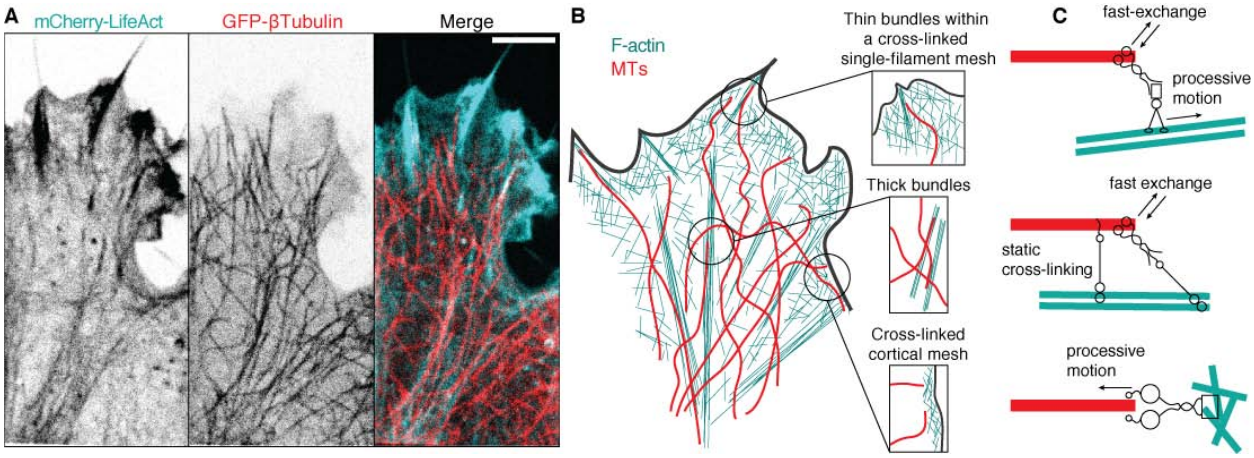

Fig. 1 *In vivo* co-organization of F-actin and microtubules.
(**A**) Fluorescence micrograph of part of a 3T3 fibroblast with fluorescent labels showing the distinct organization of F-actin (cyan) and microtubules (red). Actin forms rigid stress fibers and dense networks underneath the plasma membrane (*top*), whereas microtubules grow towards the cell periphery and form a sparse network. (**B**) Schematic showing how dynamic microtubules can encounter different F-actin architectures within a cell. (**C**) Conceptual drawings of the different types of F-actin-microtubule cross-linking proteins and protein complexes, classified based on their activities (e.g. processive motion) and exchange properties (e.g. slow *versus* fast). Scale bar: 5 µm.

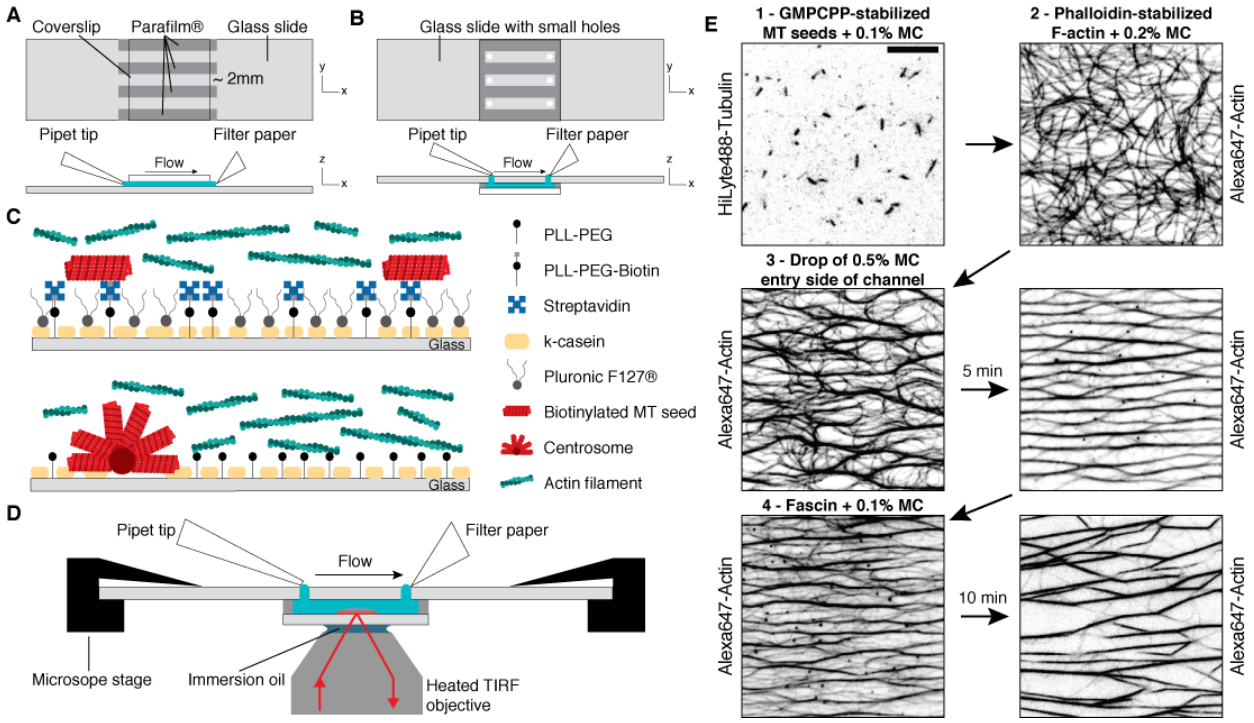

Fig. 2 Flow cell preparation and glass surface functionalization.
Schematic of the two types of flow cells we use for *in vitro* F-actin-microtubule interaction experiments with: (**A**) isotropic F-actin solutions and radial microtubule arrays, and (**B**) random arrays of microtubules and aligned F-actin-bundles. (**C**) Schematic of the surface functionalization steps for the F-actin-bundle array experiments (*Top*) and radial microtubule array experiments (*Bottom*). (**D**) Schematic of the flow cell described in (B) that can be used on a TIRF microscope stage. (**E**) TIRF images showing sequential deposition of a random array of microtubule seeds, then long actin filaments, then a methyl-cellulose (MC) solution to align and bundle the actin filaments, and finally a fascin solution to exchange MC for fascin (Section 4).

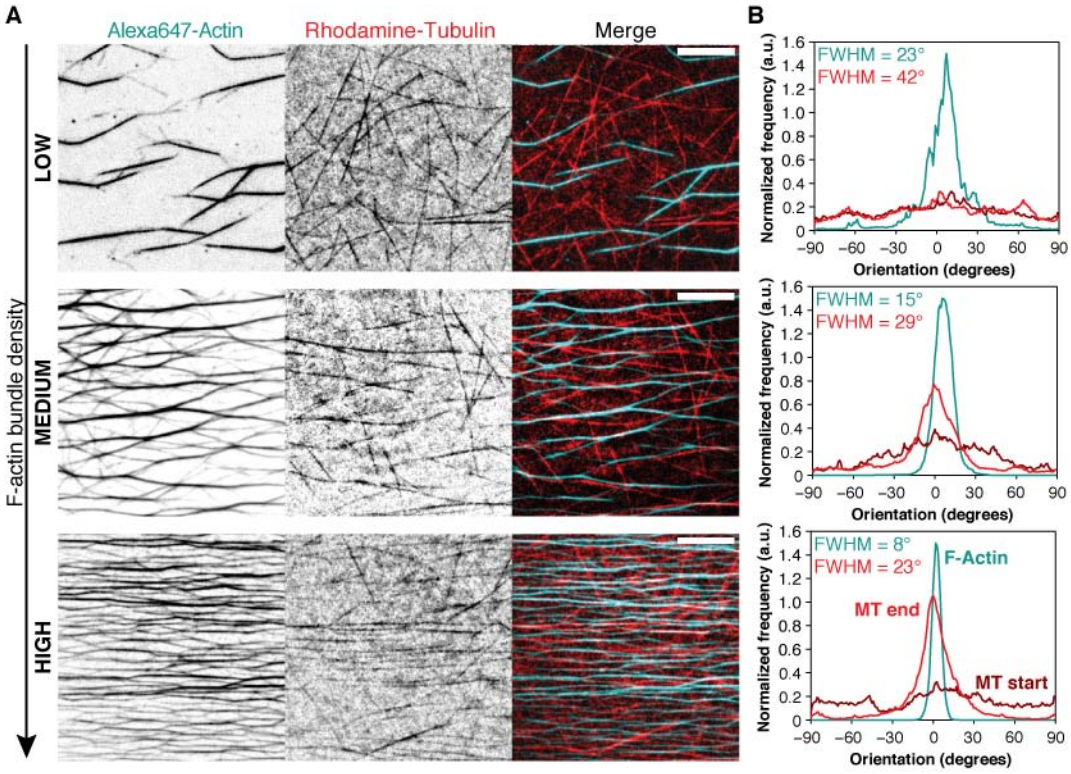

Fig. 3 TIRF images of microtubule growth within parallel arrays of F-actin bundles.
(**A**) (*Left*) Three F-actin bundle arrays of different bundle surface density. (*Middle*) Resulting microtubule arrays after 1 hr of growth within the corresponding F-actin bundle arrays. (*Right*) Merged panels. (**B**) Normalized histograms of F-actin bundle and microtubule orientation corresponding to the examples in (A). The cyan curve shows the F-actin histogram, normalized so the maximum frequency is 1.5. The dark-red curve shows the initial distribution of microtubule orientation, which is always random. The light-red curve shows the final microtubule orientation distribution after 1 hr of growth, showing that longer microtubules can be better organized by the F-actin bundles. In all graphs, the full-width at half maximum (FWHM, estimated from fitting Gaussian functions to the distributions) is shown for the F-actin bundle array as well as the resulting MT organization (light-red curves). Increasing the F-actin bundle density leads to better actin-microtubule co-alignment through steric interactions. Scale bars: 10μm.

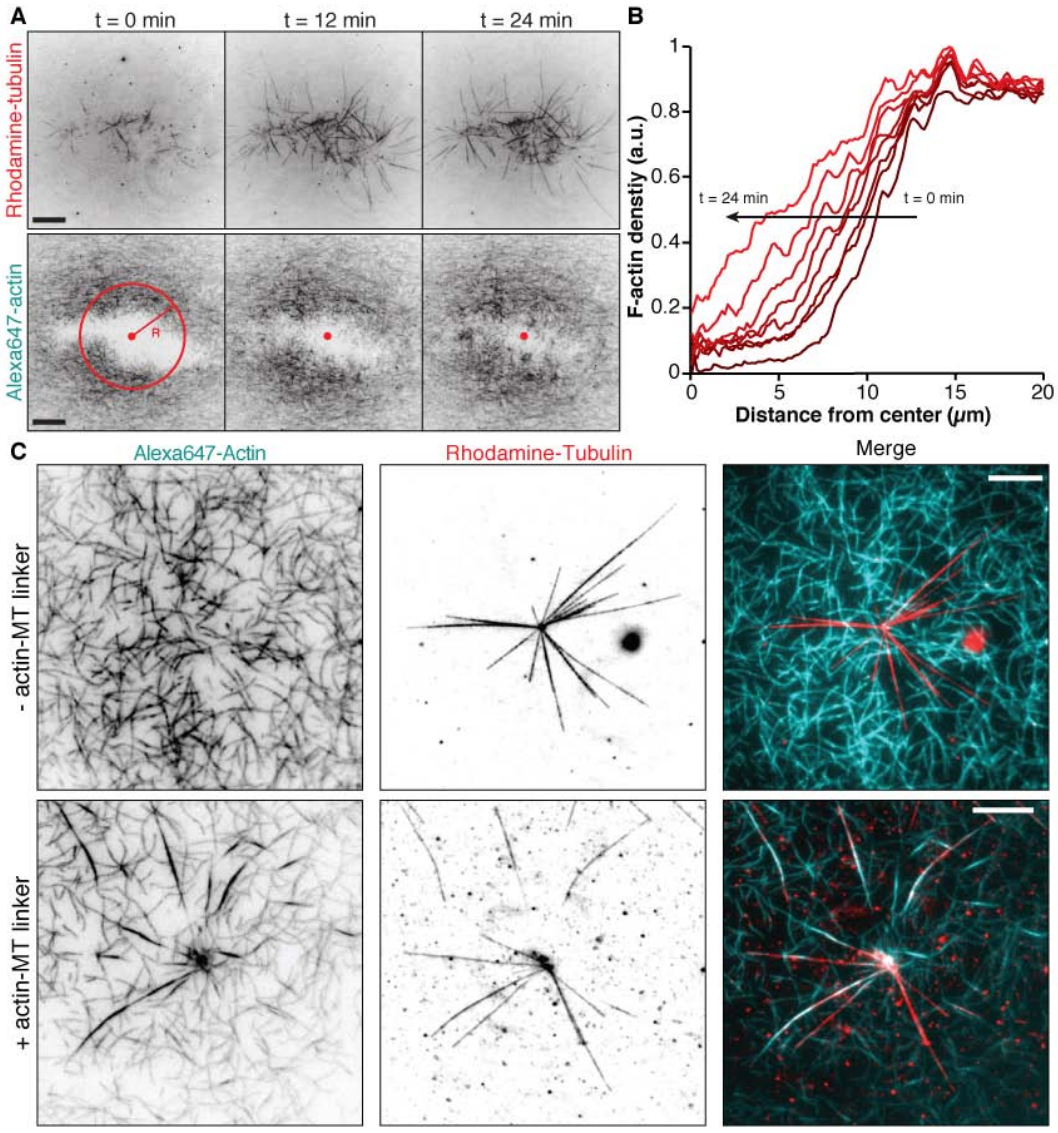

Fig. 4 TIRF images of radial microtubule growth from centrosomes within isotropic solutions of actin filaments.

(**A**) Initially we observe a zone depleted of F-actin around the centrosomes, which typically closes within 15-30 min (in this example multiple centrosomes are bound to the surface). (**B**) Radial fluorescence intensity profiles calculated at different time points demonstrate inward diffusion of actin filaments towards the centrosome cluster. (**C**) Once equilibrated, the actin filaments form a homogeneous entangled network (*Left*) that fully encloses the dynamic centrosome-based microtubule aster (*Middle*). (*Right*) Merge. (**D**) In the presence of an engineered F-actin-binding +TIP protein that binds to MT plus tips via EB, the actin filaments become radially organized as microtubules grow. Scale bars: 10μm.